AN ANALYSIS OF SKYLAB X-RAY PICTURES OF A GIANT CORONAL ARCH

STANISLAVA ŠIMBEROVÁ and MARIAN KARLICKÝ
Astronomical Institute of the Academy of Sciences of the Czech Republic, Ondřejov, Czech Republic

and

ZDENĚK ŠVESTKA
CASS, C-0111, University of California at San Diego, La Jolla, CA, U.S.A., and SRON Utrecht, The Netherlands

(Received 18 September, 1992; in revised form 10 December, 1992)

Abstract. The limb event of 13/14 August, 1973, imaged by Skylab in soft X-rays, proved to be a giant arch, quite similar to those observed in 1980–1986 on SMM. High spatial resolution (by a factor of 4–5 better than in SMM data) made it possible to see the internal structure of the arch. Its brightest part consisted of loops very similar to, but higher than, post-flare loops, surrounded by a rich system of weak loop structures extending up to altitudes of 260 000 km. While the main brightest structure of the arch was newly formed, the weak very large loops had existed above the active region before and were only enhanced during the event.

Skylab data support the model proposed by Kopp and Poletto that the giant arch is formed by reconnections high in the corona, different from the reconnection process in the underlying flare. However, contrary to Kopp and Poletto's suggestion, the data strongly indicate that the field lines that reconnect in the arch did not open before, as in the Kopp and Pneuman model: more likely, we encounter here an interaction of large-scale loops high in the corona. (The interaction of two of them is clearly seen.) Thus, while post-flare loops are formed by the Kopp and Pneuman mechanism, giant arches above eruptive flares may originate through interactive reconnections of large-scale magnetic field lines which form loops high in the corona. These loops are brought close to each other in consequence of changes in the coronal structure caused by the eruptive flare phenomenon. The arch-associated enhancement of the pre-existing large-scale active-region loops may be caused by electrons accelerated during the reconnection process and diffusing across field lines, as suggested by Achterberg and Kuipers (1984).

1. Introduction

Giant, post-flare arches were discovered in 1982 in X-ray images provided by the Hard X-ray Imaging Spectrometer (HXIS; van Beek *et al.*, 1980) aboard the SMM (Švestka *et al.*, 1982a, b; Švestka, 1984; Fárník, van Beek, and Švestka, 1986). They appear as large-scale coronal structures formed or enhanced after eruptive (two-ribbon) flares*.

These HXIS observations were made in X-rays of wavelengths below 3.5 Å. Later on, in 1984–1986, other giant arches were observed by the Flat Crystal

* 'Eruptive' flares (cf. Švestka, Jackson, and Machado, 1992) cover a broader range of phenomena than 'two-ribbon' flares, as they also include filament eruptions without any associated chromospheric flare emission (*disparitions brusques*). Some giant arches follow filament eruptions without chromospheric flares (cf. Hick, 1988), and that may also be the case in the event studied in this paper.

Solar Physics **146:** 343–356, 1993.

Spectrometer (FCS; Acton *et al.*, 1980) aboard the SMM (Hick *et al.*, 1987; Švestka, Smith, and Strong, 1992) in X-ray lines of Mg XI (9.2 Å) and O VIII (20.0 Å). Thus it appeared likely that these large-scale post-flare structures in the solar corona should also have been observed in 1973 by the soft X-ray telescope aboard Skylab which imaged the Sun in similar energy bands: 2–54 Å in the S-054, and 8–47 Å in the S-056 experiment.

In a recent *Letter to Solar Physics*, Švestka (1991) explained the problems which one encounters when checking Skylab images for large-scale coronal structures. Nevertheless, he has found at least one event in Skylab soft X-ray images which appears to be essentially the same phenomenon as the giant post-flare arches observed by the SMM. This event occurred above the western solar limb on 13 August, 1973 and was first detected at 19:16 UT by the S-046 experiment (Vorpahl, Tandberg-Hanssen, and Smith, 1977; further abbreviated as VTHS) and at 20:40 UT by the S-054 experiment (MacCombie and Rust, 1979, further abbreviated as McCR). Tandberg-Hanssen *et al.* (1975), who were the first who paid attention to this event, considered it to be a coronal condensation. Later on, Sheeley *et al.* (1975), VTHS, and McCR classified it as a long-duration X-ray event and included it among other eruptive flares with growing systems of loops.

However, the event actually has all the characteristics of the giant post-flare arches detected by the SMM, as has been demonstrated by Švestka (1991). In particular (cf. Figure 1 in Švestka's *Letter*), the time evolution of this Skylab feature (as presented in Figure 4 of VTHS) resembled almost exactly that observed in the giant arch of 6 November, 1980 (starting at 14:44 UT) observed by HXIS: maximum temperature was reached about one hour after the arch onset, maximum brightness about 2.5 hours after the onset, and maximum emission measure still one hour later. For a comparison, systems of post-flare loops (proposed as an interpretation of this event earlier by VTHS and McCR) reach maximum temperature in their onset phase and maximum emission measure only a few tens of minutes later. (See Švestka (1991) for more details.)

Thus, there can be little doubt that this was a giant post-flare arch according to its definition based on SMM data (e.g., Švestka, 1984; Hick, 1988). As a matter of fact, in their paper on this event VTHS ascribed to it many characteristic properties of giant arches when writing the following:

"For some observers, the August loop system may not qualify as a flare, since the rise time was of the order of hours rather than of minutes, and because the soft X-ray peak flux was relatively low. ...On the other hand, due to the more than 24-hour lifetime of the event, the total 8–20 Å X-ray energy of $\sim 5 \times 10^{28}$ erg was equivalent to the total X-ray energy given by others for a 'typical' flare. In fact, we will show later that $\sim 10^{30}$ erg had to be supplied to the apex of the loop system in order to explain the X-ray observations. Consequently, even though the August event may not be classified as a 'flare' as originally defined, the total energy involved was significant."

If this is compared with Švestka's (1984) analysis of the giant arch that began

at 14:44 UT on 6 November, 1980, the similarity is surprising.

According to Sheeley *et al.* (1975) a similar long-duration event (on the eastern limb) with a rise time of 3^h50^m occurred on 20 October, 1973 at 18:20 UT. Unfortunately, this was an unmanned period on Skylab so that very few data are available on that event.

2. Processing on Skylab Images

All the giant arches detected so far were observed with spatial resolution close to 0.5 arc min: 32 arc sec in the coarse field of view of HXIS and about 34 arc sec in FCS images, where we had to integrate 9 pixels to get enough counts for a statistically significant analysis (cf. Hick *et al.*, 1987). The arches are too extensive phenomena for the fine field of view of HXIS or small rasters of FCS, where spatial resolution could be enhanced. Therefore, this Skylab event offers an opportunity to analyze a giant post-flare arch with spatial resolution improved by a factor 4 or better (nominally, the angular resolution of X-ray telescopes on Skylab was about 5 arc sec close to the solar limb).

Information hidden in the Skylab images can be greatly enhanced if the images are processed, because scattered light in them has very serious deteriorating effects: its presence and steep increase with growing exposure time is probably the main reason why we have been unable to detect in Skylab data any giant arches projected on the solar disk (Švestka, 1991).

First, we began to process 16 year old, second-generation photographic copies of the event, obtained by the S-054 Skylab experiment of the AS&E through filter 1 (2–17 Å, the only images available to us). These photographs were digitized and processed using a method of local optimization of density in subimages of 33×33 pixels with a linear transformation of density (Šimberová, 1989), and results of this image processing were presented by Švestka and Šimberová (1992). In the present paper, we could use for the image processing also digitized original S-054 images of the event in filters 1 (2–17 Å) and 3 (2–54 Å) kindly provided to us by David Batchelor at NASA Data Center (GSFC)**.

From the image processing point of view this type of image poses a difficult problem. There are bright and dark objects simultaneously and the most interesting region (in our case loops above the limb) is a bright area including very smooth transitions to the background. In this case no linear or nonlinear transformation nor global methods for the processing of image data can give satisfactory results: if the dark areas become legible, the bright areas are saturated; if the bright areas become legible, the dark areas show no details.

** Unfortunately, no original digitized data could be used for the later phase of the event at 07:06 UT on August 14, because, according to Dr Batchelor, these data do not exist any more. Therefore, we had to content ourselves with the old photographs: the quality of the processed image at 07:06 UT is thus worse than at the earlier times, but still satisfactory for deducing the altitude of the brightest structure and the distance between its footpoints.

For this reason, a special algorithm for the local optimization of density has been developed. This procedure is efficient in the areas of slow transitions, but the bright and dark zones in the image stay practically on the same grid level without any specific increase of contrast. This is the reason why the processed images show the shapes of both the very bright and dark structures, but cannot reflect properly their differences in intensity from the original images.

The local area (subimage) has a circular shape and its size can be interactively changed by setting the subimage radius in pixels. In this defined local area the method of cumulative histogram has been used (see, e.g., Ballard and Brown, 1982), but the cumulative histogram was computed only to the gray level of the central pixels of the local area. Then the value of the cumulative histogram is given as

$$CH = \int_0^{S-1} h(s)\,\mathrm{d}s\,, \tag{1}$$

where s is a particular gray level in the interval 0–255, $h(s)$ the number of pixels in the subimage with that gray level, and S is the gray level of the central pixel.

Using the histogram equalization transformation, the new gray level of the central pixel is

$$CP = \frac{M}{\pi R^2} \int_0^{S-1} h(s)\,\mathrm{d}s\,, \tag{2}$$

where R is the radius of the local area in pixels and M is the number of gray levels.

The optimum enhancement of the large-scale structures which surround the giant arch is obtained by the method for local area with $R = 40$ pixels. To enhance best the giant arch, the optimal size of the local area is $R = 16$ pixels. Examples of the processed images are shown in Figures 1–3.

3. High-Resolution Images of the Arch

3.1. Coronal situation prior to the event

Figure 1 shows the situation on the western solar limb at 17:48 UT on 13 August, 1973. A filament eruption at 25° S was observed at 17:08 UT, while Sheeley *et al.* (1975) give 18:00 UT as the onset time of the X-ray brightening. Thus the limb situation pictured in Figure 1 corresponds to a time closely preceding the event studied, but after the filament eruption that was tentatively associated with it.

The processed picture in Figure 1(b) clearly shows three loops: two extending high into the corona and one at low coronal altitude. The two high loops intersect. If one compares this pre-event picture with that taken four hours later (Figure 2), one finds that the top of the brightest structure in the arch corresponds to this

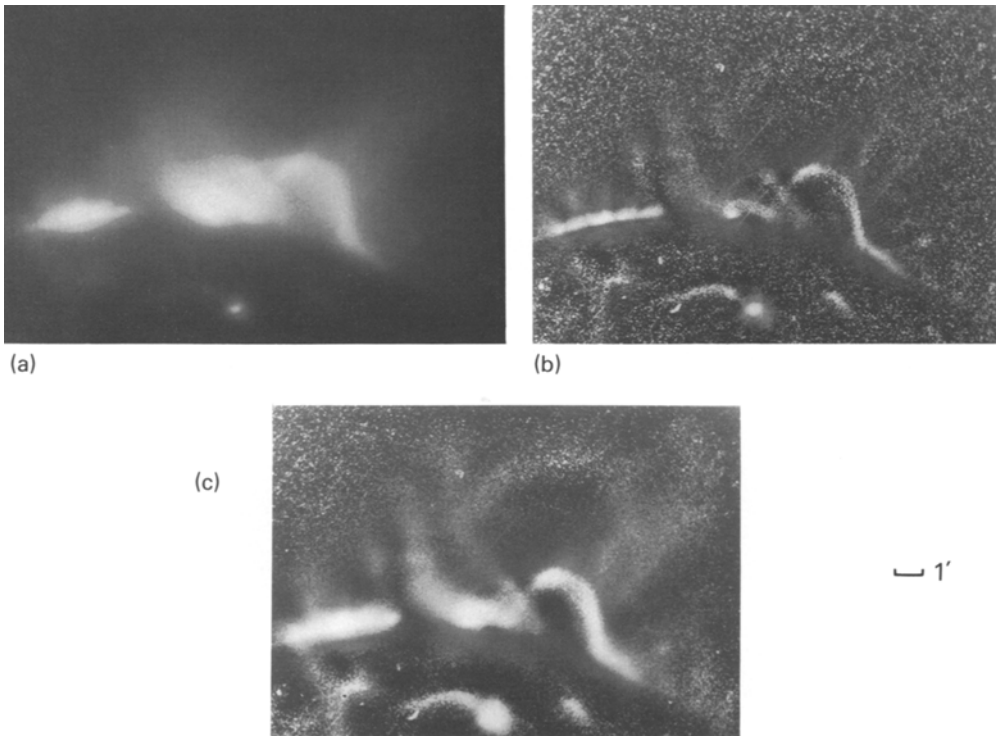

Fig. 1. X-ray images of the pre-event situation at 17:48 UT on 13 August, 1973. (In all images, west is up and north to the left.) (a) The original X-ray image in filter 1, exposure 256 s. (b) The processed image with local optimization of density in the area $R = 16$. (c) The processed image with local optimization of density in the area $R = 40$.

crossing point. During the preceding days, a roughly N–S neutral line existed at the site of the event (McCR) so that the two large-scale loops really should have been positioned close together. This offers the possibility that an interaction of large-scale loops initiated the arch, as we will discuss in Section 5.

3.2. Situation close to the maximum brightness of the arch

Figure 2 shows the situation at 21:49 UT on 13 August, close to the maximum brightness of the arch (cf. Figure 1 in Švestka (1991): the temperature peaked about one hour earlier, the emission measure about one hour later). The processed images reveal many features which could not be seen prior to the image processing and we want to draw attention, in particular, to the following ones:

(1) The brightest loop structure, which emitted most of the X-ray flux and which was interpreted by McCR as a loop-prominence system, corresponds to the lower parts of the two large loops in Figure 1 and is located exactly below the point of their apparent intersection (cf., the schematic drawing in Figure 6; Figure 2(b) actually still indicates the existence of the two loops and their crossing point).

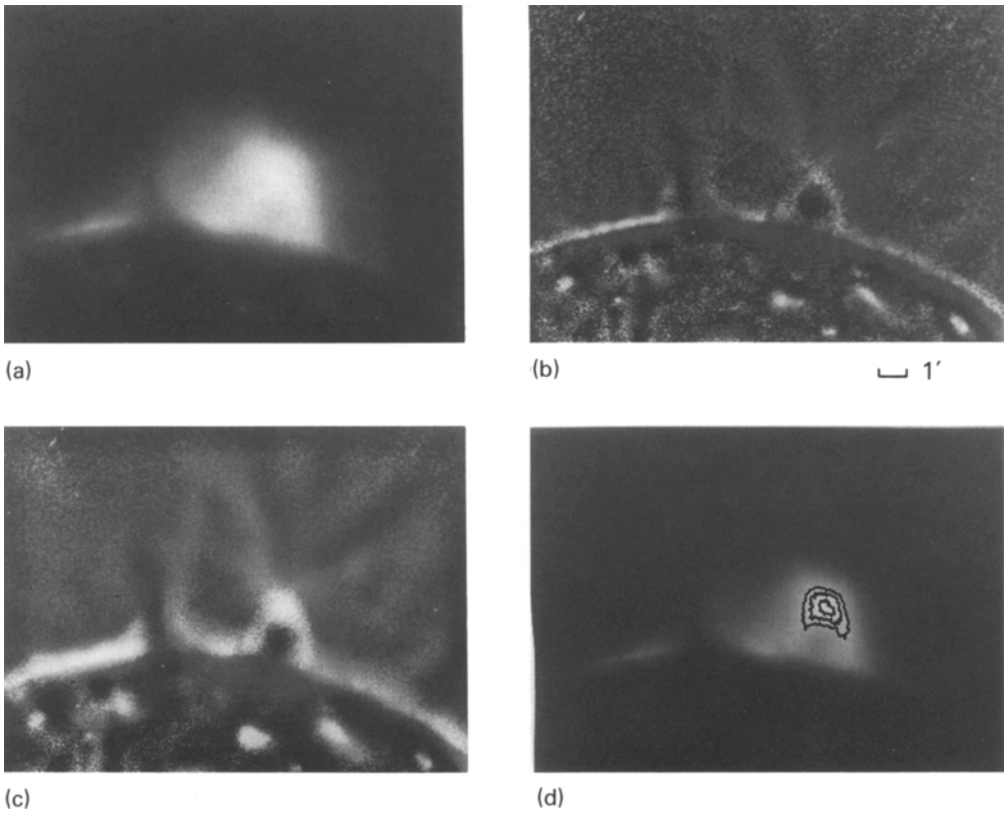

Fig. 2. X-ray images of the event near its maximum brightness at 21:49 UT on 13 August, 1973. (a) The original X-ray image in filter 3, exposure 64 s. (b) The processed image with local optimization of density in the area $R = 16$. (c) The processed image with local optimization of density in the area $R = 40$. (d) The original X-ray image in filter 3, exposure 16 s, with intensity contours at the top.

(2) The point of intersection, or the top of the brightest component of the arch, is now the brightest point in the whole arch structure (see Figures 2(c) and 2(d), in particular). McCR took this as confirmation that the observed structure was a loop prominence, because maximum brightness at the top is a characteristic feature of post-flare loops. We will explain later that this is not necessarily true.

(3) A comparison of Figures 1(b) and 2(b) shows that the bright top of the loop structure in Figure 2 is about 33 000 km higher than the intersection point in Figure 1; hence, if the bright top is identical with the intersection point, its altitude rose by 33 000 km between 17:48 UT and 21:49 UT, with average speed of 2.28 km s^{-1}. (McCR found an average speed of 0.55 km s^{-1} for the following 10 hours.)

(4) There is a very complex network of weak X-ray loops extending up to and possibly beyond an altitude of 260 000 km. These giant coronal loops extend in a variety of directions, from almost vertical ones to loops which are only slightly

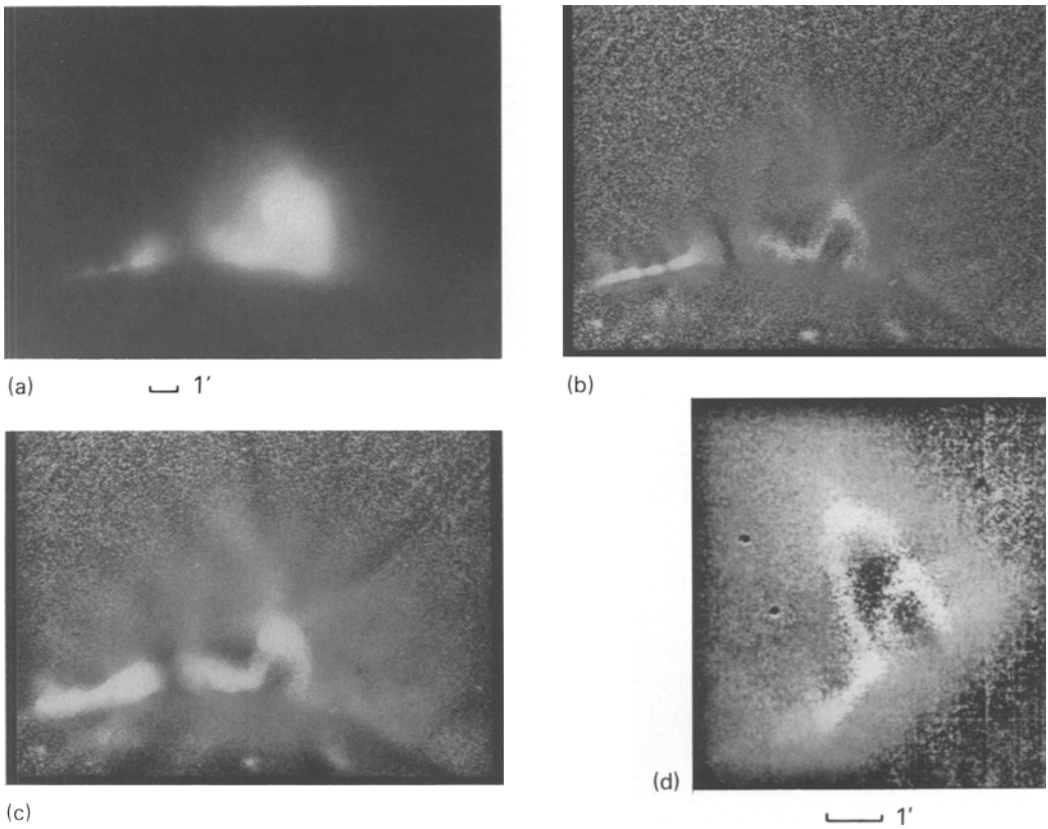

Fig. 3. X-ray images of the event at 01:00 UT (a, b, c) and 07:06 UT (d) on 14 August, 1973. (a) The original X-ray image at 01:00 UT in filter 3, exposure 64 s. (b) The processed image with local optimization of density in the area $R = 16$. (c) The processed image with local optimization of density in the area $R = 40$. (d) The processed image at 07:06 UT in filter 1, exposure 64 s, with local optimization of density in the area $R = 40$. Contrary to all the other images in Figures 1–3, this image has as its input digital data obtained from an old plane film. Note the different scale.

inclined to the surface. This configuration reminds one, on a slightly enlarged scale, of loop configurations seen in soft X-rays above other active regions (cf., e.g., Levine, 1976). Skylab X-ray images on earlier days reveal the existence of extensive loop structures above this active region (see, e.g., Švestka *et al.*, 1977).

3.3. Situation during the decay phase

Figure 3 shows the situation later on, at 01:00 UT and (in Figure 3(d)) during the decay phase, at 07:06 UT on 14 August, about 12 hours after the onset of the event. At that time one can see two bright loops, of which the higher one appears identical to that in Figures 1–3(c).

Figure 4 shows the time variation of the altitude of the top of the loop (the

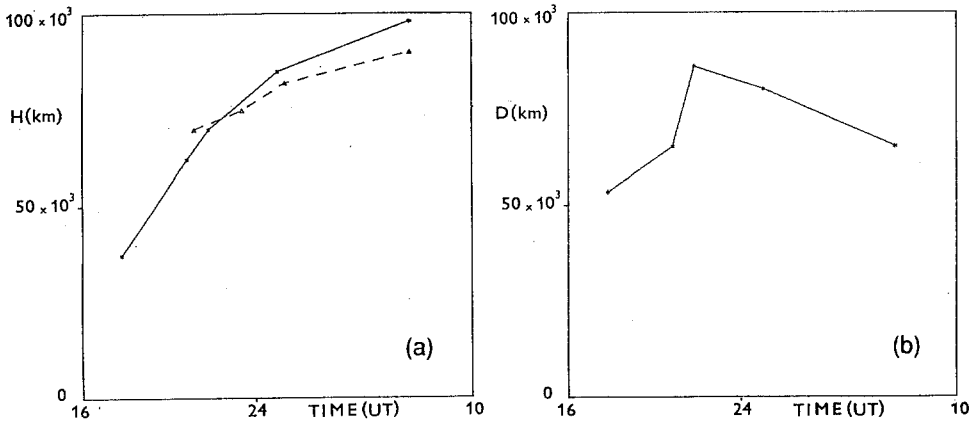

Fig. 4. (a) Time variation of the projected altitude, H, of the crossing point (top of the arch) above the limb (full line). For comparison, also the results obtained by McCR are added (dashed line). (b) Time variation of the projected distance D between the footpoints of the bright arch.

supposed crossing point) and of the distance between its footpoints. The altitude was increasing all the time, though with decreasing speed. This is what one also observes in systems of post-flare loops. The distance between the footpoints first increased as well but, starting at about 5 hours after the event onset, it began to decrease: from 86 000 km at 21:49 UT on 13 August to 80 000 km at 01:00 UT and 65 000 km at 07:06 UT on 14 August. A decrease of the footpoint distance was also noticed earlier by VTHS. This behaviour differs strikingly from the usual development of post-flare loops where the distance between footpoints (the separation of chromospheric bright ribbons) continuously increases with time. We will return to this problem in Section 5.

4. Earlier Evaluation of Skylab Data of 13/14 August, 1973

McCR published, in their Figure 2, images of the brightest loop obtained by the XUV spectrograph on Skylab in lines of He II, Ne VII, Mg IX, Fe XV, and Fe XVI, in comparison with an X-ray image between 2 and 54 Å obtained with the S-054 experiment. We present a similar figure here (Figure 5, kindly supplied by Neil Sheeley), because images in these lines have still better spatial resolution than the X-ray images and reveal quite clearly a multiple structure of thin loops of which this brightest feature above the limb was composed.

McCR found that the higher the temperature of the line formation, the higher were the imaged loops: at 01:00 UT on 14 August the Fe XV and Fe XVI loops were 3000–5000 km higher than the He II loops; this is indeed typical for loop-prominence systems (see, e.g., Švestka *et al.*, 1987). However, the same height dependence on temperature appears in any structure which is growing through successive reconnections and cooling: older, hence cooler, structures are lower than the new formed, hot ones.

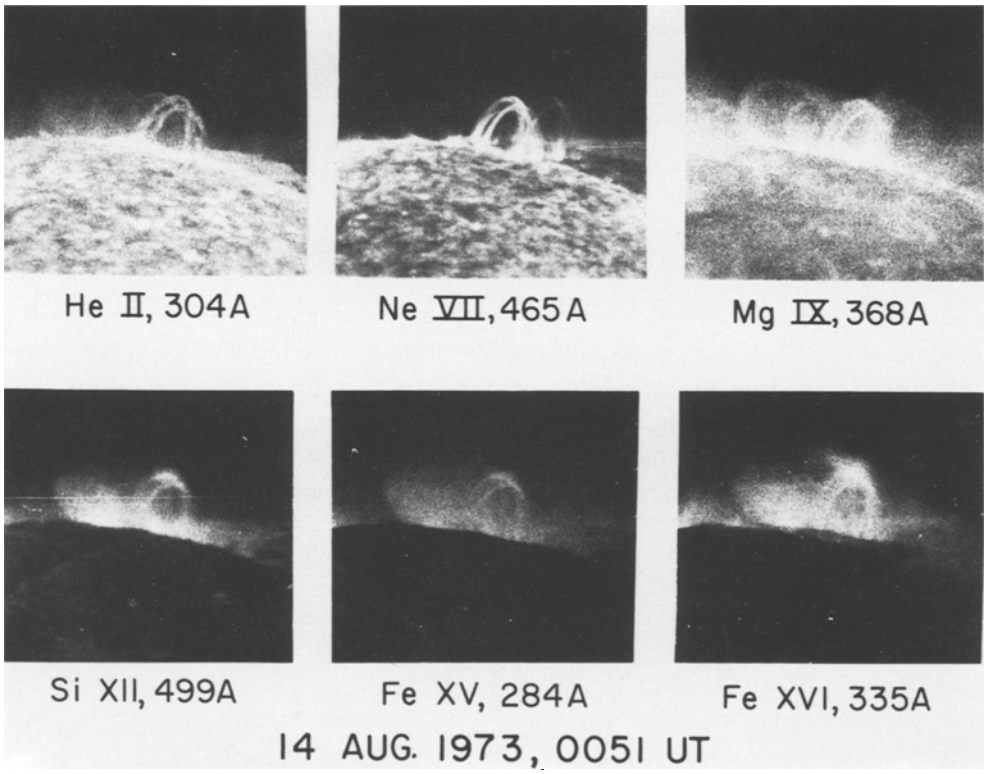

Fig. 5. Images of the event in different XUV lines at 00:51 UT on 14 August, 1973. Approximate temperatures associated with these lines range from less than 10^5 K in He II to 3×10^6 K in Fe XVI. (Courtesy of Neil Sheeley, Naval Research Laboratory, Washington, D.C.)

A second interesting feature, typical for loop-prominence systems, is the maximum of brightness at the top of the limb structure of 13/14 August. This brightness maximum is considered as evidence that post-flare loops are formed through reconnection of previously opened magnetic field lines, in the Kopp and Pneuman (1976; further abbreviated as K&P) model. Thus, it is likely that also the arch was formed through reconnection, and we will discuss this problem in Section 5. Here, however, we would like to emphasize one important difference. The maximum of brightness at the top of post-flare loops is pronounced in loops of all temperatures: from the hottest X-ray loops exceeding a temperature of 10^7 K, to the coolest Hα loops with a temperature close to 10^4 K. Here, in the 13/14 August structure, this is not the case: the maximum at the top is very pronounced in X-ray images (cf. Figures 2 and 3), it is also visible in the hot line Fe XVI, but it does not appear in the cooler lines of Mg XI, Ne VII, and He II (cf. Figure 5)

This can be explained by different electron densities, i.e., by the different role of radiative and conductive losses in the case of arch loops and post-flare loops. In both cases, the apex of the loop structures corresponds to the point of magnetic field

TABLE I

Physical parameters in the arch deduced from its soft X-ray images

Maximum	McCR	VTHS	SOLRAD
n_e	6–8 $\times$ 10^9	3.5 $\times$ 10^9	
T_e	5–6 $\times$ 10^6	6.8 $\times$ 10^6	4.5–5.5 $\times$ 10^6

reconnection. Therefore, in the arch loop, the observed maximum of X-ray radiation (Figures 2 and 3) and the maximum pressure (McCR) at this point can be explained by the energy supply from this reconnection process. After the reconnection, the arch loop is isolated from the further energy supply and starts to get colder. Further evolution of the arch loop is driven by the conductive and radiative losses.

Comparing (in ergs s^{-1}) the conductive losses

$$P_c \approx 9.4 \times 10^{26} \tag{3}$$

with the radiative losses

$$P_r \sim n_e^2 \approx 1.1 \times 10^{24} , \tag{4}$$

VTHS have shown that after the reconnection the conductive losses dominate the radiative ones. The conduction process heats the plasma to a comparable temperature throughout the whole loop and, thus, decreases the temperature gradient. This is the reason for the temperature homogeneity of older arch loops, which were visible in He II, Ne VII, and Mg XI.

In the case of post-flare loops, the situation is different. The electron density is about two orders of magnitude higher than in the case of the arch (compare, e.g., Švestka *et al.*, 1987, and Švestka, 1984). This makes the radiative losses dominate over the conductive losses. In that case the temperature gradients are not smoothed by conduction as in the case of the arch and, therefore, these gradients remain visible also during the colder phases of the post-flare loop evolution.

Both VTHS and McCR also evaluated some physical parameters in the limb structure (i.e., giant arch, as we know now). Their results are summarized in Table I.

5. Discussion

The first interpretation of giant post-flare arches was offered by Švestka *et al.* (1982a), based on the K&P model: according to these authors, the arch is the upper product of the reconnection process which creates the post-flare loops. This explained very well why only eruptive (two-ribbon) flares are followed by giant post-flare arches. A reconnection process is needed to explain the fact that the

arches can be fitted with current-free extrapolation of photospheric magnetic fields (Poletto and Kopp, 1988; Kopp and Poletto, 1990); reconnection is also indicated by the observed maximum brightness at the top of the arch structure (not only in the event studied in this paper, but also in other arches observed by HXIS, cf. Švestka *et al.*, 1982a).

However, the discovery of footpoints of the arches of 6/7 November, 1980 by Martin, Švestka, and Bhatnagar (1989) did not support this interpretation and Poletto and Kopp (1988; also see Kopp and Poletto, 1990) proposed another model: they also suppose that the arch is formed through reconnection, but this reconnection involves other field lines than those which form the post-flare loops and takes place much higher in the corona.

Poletto and Švestka (1992) proved definitely that the original interpretation by Švestka *et al.* (1982) cannot be correct: they found that one of the best observed arches began to form some 40 min before the first post-flare loops appeared. However, the other interpretation by Kopp and Poletto also meets some obstacles. Kopp and Poletto assume that the K&P mechanism can be applied both to the formation of flare loops and giant arches, though different field lines are involved in the reconnection that initiate them. It seems quite difficult to explain why two similar reconnection processes, at widely different altitudes, are accomplished at about the same time near the onsets of eruptive flares. It requires synchronized field opening of two completely different field-line systems at the onset of many eruptive flares.

Observations of the discussed Skylab event offer another possibility. We suggest that we do not encounter here reconnection of previously opened field lines, as required by K&P, but *progressive reconnection of elementary flux tubes of two (or more) interacting loops*. Two such loops are well seen in Figure 1 prior to the interaction and in Figure 2 during the reconnection process.

In the case of interacting loops, the growth at the arch can be explained by a gradual upward growth of the reconnecting loops. The longevity of the limb structure (about 50 hours according to VTHS) requires that new loop components must be formed all the time while the earlier ones cool and decay. Thus different elementary large-scale loops must subsequently reconnect and their system must gradually grow. The growth is possibly a consequence of the initial eruptive process in the active region, but note that some giant arches (like that of 21 May, 1980, cf. Švestka *et al.*, 1982) do not grow. The decrease of the arch-footpoint distance in the decay phase of the event may be due to the changing view angle of the reconnecting loops with respect to the observer in the late phase of the event.

Interacting loop models were first proposed by Gold and Hoyle (1960), and later on by Emslie (1981), Tajima *et al.* (1987), Machado *et al.* (1988), and others to explain active processes in the solar atmosphere. In our case, we assume two systems of flux tubes that interact (Figure 6, based on images in Figures 1 and 2). There may be more interacting flux tubes in the corona above the eruptive flare, but these are those two which we clearly see in projection above the solar limb prior to

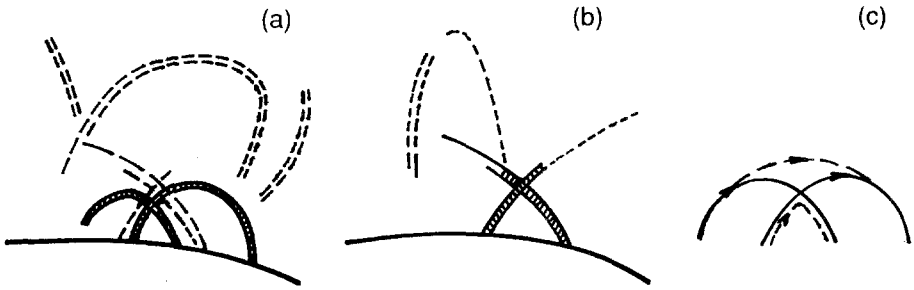

Fig. 6. Schematic drawings of the loop structure and interaction: (a) at 17:48 UT, (b) at 20:49 UT, (c) the newly formed loops (dashed).

the event. There should appear also a more extensive structure at very high altitude as the co-product of the reconnection lower in the corona (cf. Figure 6(c)), but its density (emission measure) is probably too low to make it discernible in X-rays.

Thus, generally, these Skylab observations support Kopp and Poletto's interpretation of the giant arches: a reconnection process high in the corona, different from the reconnection process which, at lower altitudes, creates the eruptive-flare loops. However, this reconnection process high in the corona is not due to the K&P mechanism of sequential reconnection of previously opened field lines: the arch is formed by interactions of large-scale loops present above the flaring active region.

This interpretation is easier to understand, and it may be more easily accomplished, than the double K&P mechanism assumed by Kopp and Poletto. If field lines open at the flare onset (in many cases giving rise to a mass ejection), this catastrophic process must certainly cause important changes in the neighboring configuration of the remaining large-scale loops above the active region that did not open and erupt. Some of them may be brought close together so that conditions for interactive reconnection are fulfilled: a giant post-flare arches begins to brighten above the active region.

Note that *this interpretation also explains why giant arches are so closely associated with eruptive flares: the eruptive process accompanying this kind of flare must lead to a powerful rearrangement of the magnetic field above the active region and, thus, provides a likely opportunity for other large-scale loops to get into contact and reconnect.* Thus the appearance of a giant arch is a likely consequence of the filament eruption. On the other hand, this interpretation does not exclude the possibility that also other kinds of flare processes could change the magnetic field configuration above an active region to that extent that reconnections of nearby large-scale loops begin to occur; thus also in the case of non-eruptive flares a structure similar to the giant arches might eventually be formed, as Mandrini and Machado (1992) believe to have seen to happen.

Figure 2 shows a rich system of large-scale loops above the active region, other than the arch itself (cf. item (4) in Section 3.2.) A comparison of the processed images prior to the event (at 17:08 UT) and near the event maximum (at 21:49 UT)

shows that these structures, or at least the brightest of them which can be recognized at 17:08 UT, were permanent active region loops existing prior to the arch brightening. As we already mentioned above, X-ray images from previous days confirm that a very rich system of high loops existed above the active region for many days (cf. Švestka *et al.*, 1977). This system of large-scale, active-region loops, however, brightened in soft X-rays in association with the arch appearance, as one can clearly see when images through the same filter, and with the same exposure time, are compared. The correct interpretation of this brightening might have been given by Achterberg and Kuipers (1984): electrons accelerated during the reconnection process diffuse across field lines and excite the neighboring, pre-existing active-region loops.

Acknowledgements

We dedicate this study to the memory of the deceased Principle Investigator of the Skylab S-054 experiment, Dr Giuseppe Vaiana. Our thanks are due to the Skylab S-054 experiment Principal Investigator Dr A. Krieger, to the software developer Dr David Batchelor, and to the National Space Science Center through the World Data Center A for Rockets and Satellites for kindly providing us with digitized images of the studied event. Dr Neil Sheeley at NRL very kindly sent us Figure 5, accompanied with helpful comments. We also thank Dr Pavel Ambrož at Ondřejov for a useful discussion.

References

Achterberg, A. and Kuipers, J.: 1984, *Astron. Astrophys.* **130**, 53.
Acton, L. W., Culhane, J. L., Gabriel, A. H., and 21 co-authors: 1980, *Solar Phys.* **65**, 53.
Ballard, D. H. and Brown, M. C.: 1982, *Computer Vision,* Preintice-Hall, Englewood Cliffs, NJ, p. 70.
Emslie, G. A.: 1981, *Astrophys. Letters* **22**, 171.
Fárník, F., van Beek, H. F., and Švestka, Z.: 1986, *Solar Phys.* **104**, 321.
Gold, T. and Hoyle, F.: 1960, *Monthly Notices Roy. Astron. Soc.* **120**, 89.
Hick, P.: 1988, 'Interpretation of Energetic Phenomena in the Solar Corona', Thesis, University Utrecht.
Hick, P., Švestka, Z., Smith, K. L., and Strong, K. T.: 1987, *Solar Phys.* **114**, 329.
Kopp, R. A. and Pneuman, G. W.: 1976, *Solar Phys.* **50**, 85.
Kopp, R. A. and Poletto, G.: 1990, *Solar Phys.* **127**, 267.
Levine, R. H.: 1976, *Solar Phys.* **46**, 159.
MacCombie, W. J. and Rust, D. M.: 1979, *Solar Phys.* **61**, 69 (abbreviated as McCR).
Machado, M. E. Moore, R. L., Hernandez, A. M., Rovira, M. G., Hagyard, M. S., and Smith, J. B.: 1988, *Astrophys. J.* **326**, 425.
Mandrini, C. H. and Machado, M. E.: 1992, *Solar Phys.* **141**, 147.
Martin, S. F., Švestka, Z., and Bhatnagar, A.: 1989, *Solar Phys.* **124**, 339.
Poletto, G. and Kopp, R. A.: 1988, *Solar Phys.* **116**, 163.
Poletto, G. and Švestka, Z.: 1992, *Solar Phys.* **138**, 189.
Sheeley, N. R., Bohlin, J. D., Brueckner, G. E., Purcell, J. D., Scherrer, V. E., Tousey, R., Smith, J. B., Speich, D. M., Tandberg-Hanssen, E., Wilson, R. M., De Loach, A. C., Hoover, R. B., and McGuire, J. P.: 1975, *Solar Phys.* **45**, 377.

Šimberová, S.: 'Numerical Methods of Data Processing in Solar Physics', Thesis, Technical University, Prague.
Solar-Geophysical Data: 1973, No. 350, Part I.
Švestka, Z.: 1984, *Solar Phys.* **94**, 171.
Švestka, Z.: 1991, *Solar Phys. (Letter)* **135**, 419.
Švestka, Z. and Šimberová, S.: 1992, *Proc. IAU Colloq.* **133**, Iguazú, *Lecture Notes in Physics* **399**, 221.
Švestka, Z., Smith, K. L., and Strong, K. T.: 1992, *Solar Phys. (Letter)* **139**, 405.
Švestka, Z., Jackson, B. V., and Machado, M. E. (eds.): 1992, *Proc. IAU Colloq.* **133**, Iguazú, *Lecture Notes in Physics* **399**.
Švestka, Z., Krieger, A. S., Chase, R. C., and Howard, R.: 1977, *Solar Phys.* **52**, 69.
Švestka, Z., Stewart, R. T., Hoyng, P., van Tend, W., Acton, L. W., Gabriel, A. H., and 8 co-authors: 1982a, *Solar Phys.* **75**, 305.
Švestka, Z., Dennis, B. R., Pick, M., Raoult, A., Rapley, C. G., Stewart, R. T., and Woodgate, B. E.: 1982b, *Solar Phys.* **80**, 143.
Švestka, Z., Fontenla, J. M., Machado, M. E., Martin, S. F., Neidig, D. F., and Poletto, G.: 1987, *Solar Phys.* **108**, 237.
Tajima, T., Sakai, J., Nakajima, H., Kosugi, T., Brunel, F., and Kundu, M. R.: 1987, *Astrophys. J.* **321**, 1031.
Tandberg-Hanssen, E., de Loach, T., Hoover, R., McGuire, J., Wilson, R., Smith, J., Speich, D., Henze, W., and Wu, S.: 1975, *Bull. Am. Astron. Soc.* **7**, 444.
Van Beek, H. F., Hoyng, P., Lafleur, B., and Simnett, G. M.: 1980, *Solar Phys.* **65**, 39.
Vorpahl, J. A., Tandberg-Hanssen, E., and Smith, J. B., Jr.: 1977, *Astrophys. J.* **212**, 550 (abbreviated as VTHS).